DMD Fast Forward. Published on January 16, 2015 as DOI: 10.1124/dmd.114.062331
This article has not been copyedited and formatted. The final version may differ from this version.

Dipeptidyl peptidase-4 greatly contributes to the hydrolysis of vildagliptin in human liver

Mitsutoshi Asakura, Hideaki Fujii, Koichiro Atsuda, Tomoo Itoh, and Ryoichi Fujiwara

Graduate School of Pharmaceutical Sciences (M.A.) and School of Pharmacy, Kitasato University, Tokyo, Japan (H.F., K.A., T.I., R.F.)

Running title: DPP-4 greatly contributes to the vildagliptin hydrolysis

Corresponding author:

Ryoichi Fujiwara, Ph.D., School of Pharmacy, Kitasato University, 5-9-1 Shirokane, Minato-ku, Tokyo 108-8641, JAPAN, fujiwarar@pharm.kitasato-u.ac.jp, +81-3-5791-6249

Number of text pages: 45

Number of tables: 2

Number of figures: 6

Number of references: 29

Number of words:

Abstract: 242

Introduction: 782

Discussion: 1,120

Abbreviations: DPP-4, dipeptidyl peptidase-4; CYP, cytochrome P450; NADPH, nicotinamide adenine dinucleotide phosphate; UGT, uridine diphosphate glucuronosyltransferase; NIT, nitrilase-like protein; HEK293, human embryonic kidney 293; Gly-Pro-AMC, H-glycyl-prolyl-7-amino-4-methylcoumarin; GAPDH, glyceraldehyde-3-phosphate dehydrogenase; BNPP, bis(*p*-nitrophenyl) phosphate; SNP, single-nucleotide polymorphism

DMD Fast Forward. Published on January 16, 2015 as DOI: 10.1124/dmd.114.062331
This article has not been copyedited and formatted. The final version may differ from this version.

Abstract

The major metabolic pathway of vildagliptin in mice, rats, dogs, and humans is hydrolysis at the cyano group to produce a carboxylic acid metabolite M20.7 (LAY151), while the major metabolic enzyme of vildagliptin has not been identified. In the present study, we determined the contribution rate of dipeptidyl peptidase-4 (DPP-4) to the hydrolysis of vildagliptin in the liver. We performed hydrolysis assay of the cyano group of vildagliptin using mouse, rat, and human liver samples. Additionally, DPP-4 activities in each liver sample were assessed by DPP-4 activity assay using the synthetic substrate Gly-Pro-AMC. M20.7 formation rates in liver microsomes were higher than those in liver cytosol. M20.7 formation rate was significantly positively correlated with the DPP-4 activity using Gly-Pro-AMC in liver samples ($r = 0.917$, $P < 0.01$). The formation of M20.7 in mouse, rat, and human liver S9 fraction was inhibited by sitagliptin, a selective DPP-4 inhibitor. These findings indicate that DPP-4 is greatly involved in vildagliptin hydrolysis in the liver. Additionally, we established stable single expression systems of human DPP-4 and its R623Q mutant, which is the non-synonymous single nucleotide polymorphism of human DPP-4, in HEK293 cells to investigate the effect of R623Q mutant on vildagliptin-hydrolyzing activity. M20.7 formation rate in HEK293 cells expressing human

DPP-4 was significantly higher than that in control HEK293 cells. Interestingly, R623Q mutation resulted in a decrease of the vildagliptin-hydrolyzing activity. Our findings might be useful for the prediction of interindividual variability in vildagliptin pharmacokinetics.

Introduction

Dipeptidyl peptidase-4 (DPP-4, CD26, EC 3.4.14.5), a serine protease belonging to type II transmembrane glycoproteins, is widely expressed on the surface of epithelial cells of diverse tissues including liver, kidney, and intestine, on endothelial cells of blood vessels, and on lymphoid cells (Mentlein, 1999; Gorrell et al., 2001). In addition to the integral membrane form, a soluble form of DPP-4 presents in serum (Durinx et al., 2000). By cleaving dipeptides from the N-terminal end of peptides and polypeptides with proline or alanine in the second position, DPP-4 controls the activity of many bioactive molecules, including incretins, cytokines, chemokines, and neuropeptides (Boonacker and Van Noorden, 2003).

Vildagliptin (LAF237) is a potent, orally active inhibitor of DPP-4 for the treatment of type 2 diabetes mellitus (Villhauer et al., 2003). DPP-4 inhibitors, so-called incretin enhancers, are attracting attention among therapeutic agents for type 2 diabetes mellitus, because they improve glucose control with a low risk of hypoglycemia (Scheen, 2010a; Deacon, 2011). While most DPP-4 inhibitors allow one single oral administration per day for management of type 2 diabetes mellitus, twice-daily administration is recommended for vildagliptin because of its shorter half-life (Deacon, 2011). Vildagliptin is extensively metabolized via at least four pathways before

excretion, with the major metabolite M20.7 (LAY151) resulting from cyano group hydrolysis (He et al., 2009a). The parent compound and the major metabolite M20.7, which is pharmacologically inactive, account for the majority of vildagliptin-related materials in human plasma (approximately 25.7 and 55%, respectively) (He et al., 2009a). Minor metabolites, which resulted from amide bond hydrolysis (M15.3), glucuronidation (M20.2), and oxidation on the pyrrolidine moiety of vildagliptin (M20.9 and M21.6), have been identified (He et al., 2009a). While 85% of an oral dose of vildagliptin is ultimately excreted by the kidney, the liver is the major site of vildagliptin metabolism in humans (He et al., 2007). Although cytochrome P450 (CYP), which is a superfamily of microsomal hemoproteins, catalyzes the reduced nicotinamide adenine dinucleotide phosphate (NADPH)-dependent oxidative metabolism of numerous drugs (Meunier et al., 2004), M20.7 was not formed by incubating vildagliptin with recombinant human CYP in the presence of NADPH (He et al., 2009a). These findings suggest that clinically relevant drug-drug interactions with vildagliptin via CYP are very unlikely (He et al., 2009a; Scheen, 2010b; He, 2012). In contrast, non-CYP enzymes, such as uridine diphosphate glucuronosyltransferase (UGT) and esterase, have attracted recent attention in pharmacokinetics, including metabolism and drug-drug interaction (Nagai, 2010; Akabane et al., 2012; Fukami and

DMD Fast Forward. Published on January 16, 2015 as DOI: 10.1124/dmd.114.062331
This article has not been copyedited and formatted. The final version may differ from this version.

Yokoi, 2012). Identification of the major metabolic enzyme responsible for vildagliptin hydrolysis is important in predicting the individual differences in pharmacokinetics and is useful for the prediction of drug-drug interactions with vildagliptin via non-CYP.

In mice, rats, dogs, and humans, the main metabolite of vildagliptin is M20.7 (He et al., 2009b). In our previous study, we investigated whether human nitrilase-like protein (NIT) 1 and NIT2, which are members of the nitrilase superfamily, are involved in the hydrolysis of vildagliptin, because the hydrolysis of the cyano group of vildagliptin is similar to nitrilase reaction (Asakura et al., 2014). However, the result of measurement of M20.7 formation rate in human embryonic kidney 293 (HEK293) cells expressing human NIT1 or NIT2 suggested that human NIT1 or NIT2 was not involved in the metabolism of vildagliptin. A previous report has shown that based on findings from the *in vivo* metabolism data in DPP-4-deficient and DPP-4-normal rats, approximately 20% of the cyano group hydrolysis reaction, which is the formation of M20.7, may be attributable to DPP-4 (He et al., 2009b). Furthermore, M20.7 was formed by incubation of vildagliptin with the recombinant human DPP-4 (He et al., 2009a). Although these data raise the possibility that DPP-4 is partially involved in formation of M20.7 in rats, contribution rate of DPP-4 to the vildagliptin hydrolysis in humans has not been clarified.

DMD Fast Forward. Published on January 16, 2015 as DOI: 10.1124/dmd.114.062331
This article has not been copyedited and formatted. The final version may differ from this version.

In the present study, we determined the contribution rate of DPP-4 to the hydrolysis of vildagliptin in the liver, which is the major site of vildagliptin hydrolysis. First, we performed hydrolysis assays of the cyano group of vildagliptin using mouse, rat, and human liver samples. Additionally, the protein expression levels of DPP-4 in each liver sample were assessed by western blot analysis. DPP-4 activities in each liver sample were also assessed by DPP-4 activity assay using the synthetic substrate H-glycyl-prolyl-7-amino-4-methylcoumarin (Gly-Pro-AMC). Second, to clarify the contribution rate of DPP-4 to the metabolism of vildagliptin, we assessed inhibitory effect of sitagliptin, a selective DPP-4 inhibitor, on vildagliptin-hydrolyzing activity of mouse, rat, and human liver S9 fractions. Finally, we established stable single expression systems of human DPP-4 and its mutants (R623Q and S630A) in HEK293 cells to assess the vildagliptin-hydrolyzing activity of human DPP-4 and to investigate the effect of the mutations on vildagliptin-hydrolyzing activity.

Materials and methods

Chemicals and reagents

DMD Fast Forward. Published on January 16, 2015 as DOI: 10.1124/dmd.114.062331
This article has not been copyedited and formatted. The final version may differ from this version.

Pooled human liver S9 fraction (50 donors, mixed gender), pooled human liver cytosol (50 donors, mixed gender), pooled rat liver S9 fraction (105 male Fischer 344 rats), pooled rat liver cytosol (105 male Fischer 344 rats), and pooled rat liver microsomes (105 male Fischer 344 rats) were obtained from XenoTech, LLC (Lenexa, KS, USA). Pooled human liver microsomes (50 donors, mixed gender) was obtained from BD Gentest (Woburn, MA, USA). AMC was purchased from Setareh Biotech, LLC (Eugene, OR, USA). Gly-Pro-AMC was obtained from Bachem (Bubendorf, Switzerland). G418 was purchased from Nacalai Tesque (Kyoto, Japan). Goat polyclonal anti-human DPP-4 antibody (AF1180) was purchased from R&D Systems (Minneapolis, MN, USA). Mouse monoclonal anti-glyceraldehyde-3-phosphate dehydrogenase (GAPDH) antibody (6C5) was purchased from American Research Products, Inc. (Belmont, MA, USA). Rabbit polyclonal anti-actin antibody (A2103), bis(*p*-nitrophenyl) phosphate (BNPP), and ethopropazine were purchased from Sigma-Aldrich (St. Louis, MO, USA). Vildagliptin was synthesized in our laboratory using the standard technique (Asakura et al., 2014). Vildagliptin carboxylic acid metabolite (M20.7) was purchased from Santa Cruz Biotechnology (Delaware Avenue, CA, USA). Sitagliptin was obtained from LKT Laboratories (St. Paul, MN, USA). All other chemicals were of the highest grade available.

DMD Fast Forward. Published on January 16, 2015 as DOI: 10.1124/dmd.114.062331
This article has not been copyedited and formatted. The final version may differ from this version.

Hydrolysis assays of the cyano group of vildagliptin

A typical incubation mixture (200 µL of total volume) contained 50 mM Tris-HCl buffer, pH 7.4, vildagliptin (1 or 10 µM), and various enzyme sources. The final concentration of mouse, rat, and human liver S9 fraction and cytosol was 1.0 mg/mL, respectively. The final concentration of mouse, rat, and human liver microsomes and S9 fraction of HEK293 cells expressing human DPP-4 or its mutants was 0.5 mg/mL, respectively. Mouse liver S9 fraction, cytosol, and microsomes were prepared previously (Asakura et al., 2014). The reaction was initiated by adding vildagliptin after a 5 min preincubation at 37 °C. After incubation at 37 °C for 2 h, the reaction was terminated by an addition of 200 µL of cold acetonitrile. After removal of protein by centrifugation at 15,000 g for 5 min, a 50-µL portion of the sample was subjected to liquid chromatography/tandem mass spectrometry (LC-MS/MS) assay to measure the concentration of M20.7. The non-reaction control samples were kept on ice for the full period before centrifugation. The concentration of M20.7 obtained with the non-reaction control was subtracted from that obtained with each enzyme source. The vildagliptin-hydrolyzing activity was expressed as an M20.7 formation rate (pmol/h/mg protein).

LC-MS/MS conditions

A Waters Micromass tandem quadrupole Quattro micro mass spectrometer (Waters, Milford, MA, USA) was interfaced with a Waters Alliance 2695 Separation Module (Waters) via an electrospray ionization probe in the positive ion mode. M20.7 was separated on a Polaris 5 µm C18-A 50 × 2.0-mm column (25 °C) (Agilent Technologies, Amstelveen, The Netherlands) with a MetaGuard 2.0 mm Polaris 5 µm C18-A guard column (Agilent Technologies). The mobile phase of A/B (1:3, v/v) was used, where A was methanol/10 mM ammonium acetate, pH 8.0 (5:95, v/v), and B was acetonitrile/methanol (10:90, v/v). The flow rate was adjusted to 0.2 mL/min, and an eluent between 0 and 5 min was introduced into the mass spectrometer. The ionization conditions were as follows: capillary voltage, 3.6 kV; cone voltage, 32 V; collision energy, 20 V; sourcetemperature, 120 °C; desolvationtemperature, 400 °C; collision gas, argon. The sample was analyzed during the multiple reaction monitoring mode of the mass spectrometer at a dwell time of 0.5 s per channel using m/z 323.1 > 173.3 as the transition.

DPP-4 activity assays

DPP-4 activity was determined by cleavage rate of AMC from the synthetic substrate Gly-Pro-AMC (Leiting et al., 2003; Lee et al., 2009). These assays were performed in 96-well flat-bottom plates in a total assay volume of 100 µL. The diluted enzyme sources (0.5 to 40

DMD Fast Forward. Published on January 16, 2015 as DOI: 10.1124/dmd.114.062331
This article has not been copyedited and formatted. The final version may differ from this version.

μg/mL) were incubated for 15 min at room temperature in assay buffer (50 mM glycine, pH 8.7, 1 mM EDTA). After 15 min incubation, Gly-Pro-AMC was added. The final concentration of Gly-Pro-AMC was 50 μM. The plates were incubated at 25 °C for 10 min. After incubation, fluorescence was measured using a SpectraMax M5 96-well plate spectrophotometer (excitation, 360 nm; emission, 460 nm, Molecular Devices, Sunnyvale, CA, USA). The standard curve of free AMC was constructed using 0 to 10 μM solutions of AMC. The DPP-4 activity was expressed as the amount of cleaved AMC per minute per mg protein (nmol/min/mg protein).

SDS-PAGE and western blot analysis

Mouse liver samples (100 μg of protein), rat liver samples (100 μg of protein), human liver samples (100 μg of protein), and cell S9 fractions (3 μg of protein) were subjected to NuPAGE 4-12% Bis-Tris Gel (Lifetechnologies, Carlsbad, CA, USA) and transferred to a PVDF membrane Immobilon-P (Millipore, Bedford, MA, USA) following the manufacurer's protocol. The membrane was blocked for 1 h with 50 mg/mL skimmed milk in phosphate buffered saline (PBS) and then incubated with anti-human DPP-4 antibody (AF1180) diluted with PBS (1:1,000) as a primary antibody overnight. The membrane was washed with PBS three times and incubated with HRP-labeled secondary antibody diluted with PBS (1:10,000) for 1 h. The bands were

detected using Chemi-Lumi One L Western-blotting detection reagents (Nacalai Tesque). Anti-GAPDH antibody (1:5,000) or anti-Actin antibody (1:5,000) was used as the protein loading control.

Inhibition study of vildagliptin-hydrolyzing activity

The inhibitory effect of sitagliptin, a selective DPP-4 inhibitor, on vildagliptin-hydrolyzing activity was investigated using mouse, rat, and human liver S9 fraction as an enzyme source. The inhibitory effect of bis(*p*-nitrophenyl) phosphate and ethopropazine, a carboxylesterase and butyrylcholinesterase inhibitor, respectively, on vildagliptin-hydrolyzing activity of human liver S9 fractions was also investigated. Vildagliptin (10 μM) and inhibitors (10, 100, and 1000 μM) were incubated with the each liver S9 fraction at 1.0 mg/mL. In the presence of the inhibitor, vildagliptin-hydrolyzing activity was measured as described above.

Expression of human DPP-4 in HEK293 cells and mutant construction

Human *DPP-4* (National Center for Biotechnology Information (NCBI) accession number NM_001935.3) cDNA were prepared by a reverse transcription-polymerase chain reaction technique from human liver total RNA with sense and antisense oligonucleotide primers (5'-TGT

DMD Fast Forward. Published on January 16, 2015 as DOI: 10.1124/dmd.114.062331
This article has not been copyedited and formatted. The final version may differ from this version.

TTA ACT CGG GGC CGA AA-3' and 5'-CAG ACC AGG ACC GGA ACA TC-3' for DPP-4 vector 1; 5'-GTT GGA AGA TTT AGG CCT TCA GA-3' and 5'-CCC TAG TGA CAT CAC TGC CC-3' for DPP-4 vector 2). The PCR products were subcloned into pTARGET Mammalian Expression Vector (Promega, Madison, WI, USA) and the DNA sequences of the inserts were determined by a BigDye Terminator v3.1 cycle sequencing kit (Applied Biosystems, Foster City, CA, USA) using a 3130 Genetic Analyzer (Applied Biosystems). The two vectors, DPP-4 vector 1 and DPP-4 vector 2, have two *Stu*I sites, respectively (Supplemental Fig. 1). To construct the expression vector of full-length human DPP-4, we subcloned the 2.95-kb *Stu*I fragment of DPP-4 vector 2 into the 5.56-kb *Stu*I fragment of DPP-4 vector 1. Additionally, we constructed the two expression vectors of human DPP-4 mutant. The expression vector of DPP-4 vector 2 was used as the template for constructing mutants. A KOD-plus-Neo DNA polymerase (Toyobo, Osaka, Japan) was used to create two single mutants of human DPP-4 (R623Q or S630A) in this study. The forward and reverse primers used for the mutagenesis were shown as follows: 5'-CAA CAA ACA AAT TGC AAT TTG GGG CTG GTC-3' and 5'-CCC AAA TTG CAA TTT GTT TGT TGT CCA CAA ATC CC-3' for the R623Q mutant, and 5'-GCA ATT TGG GGC TGG GCA TAT GGA GGG TAC GTA ACC-3' and 5'-GGT TAC GTA CCC TCC ATA TGC CCA GCC

DMD Fast Forward. Published on January 16, 2015 as DOI: 10.1124/dmd.114.062331
This article has not been copyedited and formatted. The final version may differ from this version.

CCA AAT TGC-3' for the S630A mutant. To construct the expression vector of full-length R623Q or S630A, we subcloned the 2.95-kb *Stu*I fragment of DPP-4 vector 2 mutated R623Q or S630A into the 5.56-kb *Stu*I fragment of DPP-4 vector 1, respectively. To confirm the desired mutation and verify the absence of unintended mutations, the constructs were sequenced.

HEK293 cells were obtained from the Cell Resource Center for Biomedical Research, Tohoku University (Sendai, Japan). The cells were grown in Dulbecco's modified Eagle's medium containing 100 U/mL penicillin, 100 μg/mL streptomycin, and 10% fetal bovine serum with 5% CO_2 at 37 °C. The wild-type human DPP-4-, R623Q-, or S630A-expressing HEK293 cells and control cells (Mock) were constructed by transfecting the expression vector and control pTARGET vector, respectively, into cells using a Lipofectamine LTX & Plus Reagent (Invitrogen, Carlsbad, CA, USA). Stable transfectants were selected in medium containing 600 μg/mL G418 and several clones were isolated.

Preparation of cell S9 fraction

HEK293 cells expressing single wild-type human DPP-4, R623Q, or S630A was suspended in cold PBS and homogenized with a teflon-glass homogenizer for 40 strokes. The total cell

DMD Fast Forward. Published on January 16, 2015 as DOI: 10.1124/dmd.114.062331
This article has not been copyedited and formatted. The final version may differ from this version.

homogenate was centrifuged at 600 g for 10 min at 4 °C. The pellet, which contained nuclear, was discarded. The supernatant, which contained mostly cell protein, was collected as the cell homogenate. Additionally, the cell homogenate was centrifuged at 9,000 g for 20 min at 4 °C. The supernatant was used as the S9 fraction.

Kinetic analysis of DPP-4 activity and vildagliptin-hydrolyzing activity

The kinetic analysis of DPP-4 activity using the synthetic substrate Gly-Pro-AMC was performed using human liver samples, human DPP-4-expressing HEK293 cells, and DPP-4 mutant-expressing HEK293 cells with substrate concentrations from 10 to 200 μM. The kinetic analysis of vildagliptin-hydrolyzing activity was performed using human liver samples with substrate concentrations from 1 to 1000 μM and using HEK293 cells expressing human DPP-4 and its mutants with substrate concentrations 1 to 500 μM, respectively. Kinetic parameters were estimated from the fitted curves using a KaleidaGraph computer program (Synergy Software, Reading, PA, USA) designed for nonlinear regression analysis. The following equations were applied for Michaelis-Menten kinetics (eq. 1) or biphasic kinetics (eq. 2):

$$V = V_{max} \times S/ (K_m + S) \quad (1)$$

DMD Fast Forward. Published on January 16, 2015 as DOI: 10.1124/dmd.114.062331
This article has not been copyedited and formatted. The final version may differ from this version.

$$V = V_{max1} \times S/ (K_{m1} + S) + V_{max2} \times S/ (K_{m2} + S) \quad (2)$$

where V is the initial velocity of the reaction, V_{max} is the maximum velocity, S is the substrate concentration, and K_m is the Michaelis constant, which is defined as the substrate concentration at one-half the maximum velocity. K_{m1} and K_{m2} are affinity constants for high and low-affinity sites, respectively, and V_{max1} and V_{max2} are maximum velocities for high and low-affinity sites, respectively. Kinetic data were also analyzed using Eadie-Hofstee plots.

Statistical analysis

Data were presented as means ± S.D. and were assessed for statistical significance using the unpaired t-test. The correlation analysis was preformed using the Spearman rank method. A value of $P < 0.05$ was considered statistically significant.

Results

Vildagliptin-hydrolyzing activity of mouse, rat, and human liver samples

DMD Fast Forward. Published on January 16, 2015 as DOI: 10.1124/dmd.114.062331
This article has not been copyedited and formatted. The final version may differ from this version.

M20.7 formation rates in mouse, rat, and human liver samples were measured. Time and protein linearity studies were performed using human liver S9 fraction. It was demonstrated that formation of M20.7 in human liver S9 fraction increased linearly for at least 2 h and 2.0 mg/mL, respectively (data not shown). M20.7 formation rate in human liver S9 fraction, cytosol, and microsomes was 0.21 ± 0.03, 0.13 ± 0.01, and 0.64 ± 0.05 pmol/h/mg protein, respectively, at a substrate concentration of 10 μM (Fig. 1A). M20.7 formation rate in human liver microsomes was statistically higher than that in the liver cytosol ($P < 0.01$). M20.7 formation rate in mouse liver S9 fraction, cytosol, and microsomes was 0.41 ± 0.04, 0.36 ± 0.01, and 0.51 ± 0.02 pmol/h/mg protein, respectively. M20.7 formation rate in rat liver S9 fraction, cytosol, and microsomes was 0.50 ± 0.01, 0.32 ± 0.02, and 0.95 ± 0.03 pmol/h/mg protein, respectively. M20.7 formation rate in mouse and rat liver microsomes was also statistically higher than that in the liver cytosol, respectively ($P < 0.01$). These results indicate that the cyano group hydrolysis reaction of vildagliptin can be catalyzed by enzymes present in the liver, particularly in liver microsomes. A kinetic analysis of vildagliptin-hydrolyzing activity was performed using human liver samples (Fig. 1B). The Eadie-Hofstee plots of vildagliptin-hydrolyzing activities in human liver S9 fraction, cytosol, and microsomes were not linear at the low substrate concentration, indicating

DMD Fast Forward. Published on January 16, 2015 as DOI: 10.1124/dmd.114.062331
This article has not been copyedited and formatted. The final version may differ from this version.

that multiple enzymes might be responsible for the hydrolysis of vildagliptin (Supplemental Fig. 2A). Because the kinetic parameters of human liver samples could not been calculated using the KaleidaGraph computer program, these parameters were calculated from the Eadie-Hofstee plots (Supplemental Fig. 2A). The K_m value for high-affinity sites of the vildagliptin-hydrolyzing activity in human liver S9 fraction, cytosol, and microsomes was 1.95 ± 0.6, 2.34 ± 1.0, and 0.75 ± 0.4 μM, respectively (Table 1). The K_m value for low-affinity sites of the vildagliptin-hydrolyzing activity in human liver S9 fraction, cytosol, and microsomes was 335 ± 10, 189 ± 5.0, and 448 ± 104 μM, respectively (Table 1).

DPP-4 activities and protein expression levels of DPP-4 in mouse, rat, and human liver samples

We performed DPP-4 activity assay using Gly-Pro-AMC, which is a synthetic DPP-4-specific substrate (Leiting et al., 2003; Lee et al., 2009), and western blot analysis using mouse, rat, and human liver samples. The DPP-4 activity in human liver S9 fraction, cytosol, and microsomes was 1.9 ± 0.2, 1.4 ± 0.2, and 3.3 ± 0.1 nmol/min/mg protein, respectively, at a substrate concentration of 50 μM (Fig. 2A). The DPP-4 activity in human liver microsomes was statistically higher than that in the liver cytosol ($P < 0.01$). Additionally, DPP-4 activity in mouse

DMD Fast Forward. Published on January 16, 2015 as DOI: 10.1124/dmd.114.062331
This article has not been copyedited and formatted. The final version may differ from this version.

and rat liver microsomes was also statistically higher than that in the liver cytosol, respectively. These results suggest that DPP-4 is abundantly present in liver microsomes. Indeed, the protein of DPP-4 was highly detected in liver microsomes (Fig. 2B). The protein expression level of DPP-4 in liver samples correlated well with the DPP-4 activity in each liver sample (Fig. 2A and 2B). A kinetic analysis of the DPP-4 activity was performed using human liver samples. The DPP-4 activity by human liver S9 fraction, cytosol, and microsomes followed the Michaelis-Menten equation (Fig. 2C), as the Eadie-Hofstee plots were almost linear, respectively (Supplemental Fig. 3A). The K_m value of the DPP-4 activity in human liver S9 fraction, cytosol, and microsomes was 26.2 ± 2.5, 21.3 ± 1.5, and 24.6 ± 1.1 μM, respectively (Table 2).

We further preformed correlation analyses between M20.7 formation rates and DPP-4 activities in the liver samples (Fig. 3). M20.7 formation rate was significantly positively correlated with the DPP-4 activity using Gly-Pro-AMC in liver samples (r = 0.917, P < 0.01). This finding suggests that DPP-4 is primarily responsible for vildagliptin hydrolysis in the liver.

Inhibition study of vildagliptin-hydrolyzing activity

The inhibitory effect of sitagliptin, a selective DPP-4 inhibitor, on vildagliptin-hydrolyzing activity of mouse, rat, and human liver S9 fractions was assessed. The formation of M20.7 was

DMD Fast Forward. Published on January 16, 2015 as DOI: 10.1124/dmd.114.062331
This article has not been copyedited and formatted. The final version may differ from this version.

inhibited by sitagliptin in a concentration-dependent manner (Fig. 4A). The formation of M20.7 in human liver S9 fraction was approximately 60% inhibited by 1000 μM sitagliptin. The formation of M20.7 in mouse and rat liver S9 fraction was approximately 50 and 90% inhibited by 1000 μM sitagliptin, respectively.

We also assessed inhibitory effect of BNPP (a carboxylesterase inhibitor) and ethopropazine (a butyrylcholinesterase inhibitor) on vildagliptin-hydrolyzing activity of human liver S9 fractions, because it has been reported that anagliptin, which has the same cyanopyrrolidine motif as vildagliptin, is metabolism by DPP-4, carboxylesterase, and butyrylcholinesterase (Furuta et al., 2013). However, the formation of M20.7 in human liver S9 fraction was not inhibited by BNPP and ethopropazine (Fig. 4B). These results indicate that DPP-4 is greatly involved in vildagliptin hydrolysis in mouse, rat, and human liver, whereas carboxylesterase and butyrylcholinesterase is not involved in vildagliptin hydrolysis in human liver.

Establishment of single expression systems of wild-type human DPP-4, R623Q, and S630A in HEK293 cells

To assess the vildagliptin-hydrolyzing activity of human DPP-4, we constructed the stable single expression systems of wild-type human DPP-4 in HEK293 cells (HEK/DPP-4). To assess

DMD Fast Forward. Published on January 16, 2015 as DOI: 10.1124/dmd.114.062331
This article has not been copyedited and formatted. The final version may differ from this version.

the effects of two DPP-4 mutants on DPP-4 activity and vildagliptin-hydrolyzing activity, stable single expression systems of R623Q and S630A in HEK293 cells (HEK/R623Q and HEK/S630A) were also constructed. R623Q (rs147614497) is the non-synonymous human DPP-4 single-nucleotide polymorphism (SNP) with the highest minor allele frequency (MAF = 0.0248) in December 2013, which has been reported in the NCBI dbSNP (build 141; http://www.ncbi.nlm.nih.gov/projects/SNP/). S630A is an active site mutant that lacked the catalytic serine 630 residue required for DPP-4 activity (Tanaka et al., 1993; Metzler et al., 2008; Greene et al., 2011). The protein expression levels of DPP-4 were assessed by western blot analysis. We selected the clones with the highest DPP-4 protein levels for the subsequent analyses. Significant DPP-4 protein expression was observed in the cell S9 fraction of the wild-type human DPP-4-transfectant compared with that of Mock cells (Fig. 5A). The R623Q- or S630A-transfectant also showed significant DPP-4 protein expression compared with Mock, respectively. In addition, the protein expression levels of DPP-4 in HEK/R623Q and HEK/S630A were similar and higher than that in HEK/DPP-4, respectively. The two bands reacting with the anti-human DPP-4 antibody were observed in HEK/DPP-4 and HEK/R623Q. To elucidate whether the two bands were different glycosylation forms of DPP-4, the S9 fraction of

DMD Fast Forward. Published on January 16, 2015 as DOI: 10.1124/dmd.114.062331
This article has not been copyedited and formatted. The final version may differ from this version.

HEK/DPP-4 was deglycosylated under denaturing conditions and analyzed by western blotting with the anti-human DPP-4 antibody. Glycosidase treatment reduced the size of two bands to a single 110-kDa band in HEK/DPP-4 (Supplemental Fig. 4). This result suggested that the two bands reacting with the anti-human DPP-4 antibody in HEK/DPP-4 and HEK/R623Q were different glycosylation forms of DPP-4.

Effects of DPP-4 mutants on DPP-4 activity

To assess the DPP-4 activity of wild-type human DPP-4, we performed DPP-4 activity assays using the synthetic substrate Gly-Pro-AMC. To assess the effects of R623Q and S630A on DPP-4 activity, we also performed DPP-4 activity assays using HEK/R623Q and HEK/S630A. The DPP-4 activity in Mock, HEK/DPP-4, HEK/R623Q, and HEK/S630A was 1.2 ± 0.1, 134 ± 5.3, 132 ± 6.2, and 1.0 ± 0.1 nmol/min/mg protein, respectively, at a substrate concentration of 50 μM (Fig. 5B). The DPP-4 activity in HEK/DPP-4 was approximately 100- fold higher than that in Mock. The DPP-4 activity in HEK/R623Q was comparable with that in HEK/DPP-4. Although S630A-transfectant showed significant DPP-4 protein expression compared with Mock, the DPP-4 activity in HEK/S630A was comparable with that in Mock. A kinetic analysis of DPP-4 activity was performed using Mock, HEK/DPP-4, and HEK/R623Q. The DPP-4 activity in

DMD Fast Forward. Published on January 16, 2015 as DOI: 10.1124/dmd.114.062331
This article has not been copyedited and formatted. The final version may differ from this version.

recombinant human DPP-4 (hDPP-4) and R623Q (hR623Q) was expressed as the DPP-4 activity (nmol/min/mg protein) in which the DPP-4 activity obtained with Mock was subtracted from that obtained with HEK/DPP-4 and HEK/R623Q, respectively. The DPP-4 activity by wild-type hDPP-4 and hR623Q followed the Michaelis-Menten equation (Fig. 5C), as the Eadie-Hofstee plots were almost linear, respectively (Supplemental Fig. 3B). The K_m value of the DPP-4 activity in wild-type hDPP-4 and hR623Q was 54.0 ± 2.6 and 45.6 ± 8.0 μM, respectively (Table 2). The K_m value of the DPP-4 activity in hR623Q was close to that in wild-type hDPP-4.

Effects of DPP-4 mutants on vildagliptin-hydrolyzing activity

To assess the vildagliptin-hydrolyzing activity of wild-type human DPP-4, we performed hydrolysis assays of the cyano group of vildagliptin using HEK/DPP-4. To assess the effects of R623Q and S630A on vildagliptin-hydrolyzing activity, we also performed hydrolysis assays of the cyano group of vildagliptin using HEK/R623Q and HEK/S630A. The M20.7 formation rate in Mock, HEK/DPP-4, HEK/R623Q, and HEK/S630A was 0.18 ± 0.01, 7.4 ± 0.2, 5.2 ± 0.1, and 0.13 ± 0.01 pmol/h/mg protein, respectively, at a substrate concentration of 1 μM (Fig. 5D). The M20.7 formation rate in HEK/DPP-4 was statistically higher than that in Mock ($P < 0.01$). Interestingly, although DPP-4 activity in HEK/R623Q was comparable with that in HEK/DPP-4,

M20.7 formation rate in HEK/R623Q was statistically lower than that in HEK/DPP-4 ($P < 0.01$). Furthermore, M20.7 formation rate in HEK/S630A was comparable with that in Mock. These results suggest that the catalytic serine 630 residue is directly involved in the vildagliptin hydrolysis in human DPP-4 and that R623Q mutation results in a decrease of the vildagliptin-hydrolyzing activity. A kinetic analysis of vildagliptin-hydrolyzing activity was performed using Mock and HEK/DPP-4. The vildagliptin-hydrolyzing activity in hDPP-4 was expressed as an M20.7 formation rate (pmol/h/mg protein) in which the vildagliptin-hydrolyzing activity obtained with Mock was subtracted from that obtained with HEK/DPP-4. Because the vildagliptin-hydrolyzing activity in Mock at the high substrate concentration was higher than that in HEK/R623Q, the parameters of hR623Q could not been calculated. The vildagliptin-hydrolyzing activity by hDPP-4 followed the biphasic equation (Fig. 5E), as the Eadie-Hofstee plots were biphasic (Supplemental Fig. 2B). The K_m value for high and low-affinity sites of vildagliptin-hydrolyzing activity in hDPP-4 was 0.62 ± 0.1 and 151 ± 71 μM, respectively (Table 1). The K_m value for high-affinity site of vildagliptin-hydrolyzing activity in hDPP-4 was similar to that in human liver samples.

Discussion

Identification of major enzyme responsible for the metabolism of drugs is important to understand interindividual variability in pharmacokinetics. In the present study, we clarified the contribution rate of DPP-4 to the cyano group hydrolysis reaction of vildagliptin in mouse, rat, and human liver. The results of correlation analysis (Fig. 3) and inhibition study (Fig. 4A) indicated that DPP-4 was greatly involved in vildagliptin hydrolysis in mouse, rat, and human liver (Fig. 6). The formation of M20.7 in HEK/DPP-4 was approximately 90% inhibited by 1000 μM sitagliptin (Supplemental Fig. 5), indicating that the concentration of sitagliptin was adequate for inhibition of vildagliptin-hydrolyzing activity in human DPP-4. Therefore, the results of inhibition study suggest that the contribution rate of DPP-4 to vildagliptin hydrolysis in human liver is approximately 60% (Fig. 4A). To predict the *in vivo* clearance of vildagliptin, plasma protein binding and affinity of vildagliptin for DPP-4 are also important factors. While the affinity of vildagliptin for DPP-4 is high, binding of vildagliptin to plasma proteins is very low (9.3%) (He et al., 2009a). Therefore, it has been suggested that protein binding of vildagliptin is clinically negligible (He et al., 2009a; Golightly et al., 2012). Additionally, to understand the DPP-4 protein expression in various tissues, we performed western blot analysis using 8 mouse

DMD Fast Forward. Published on January 16, 2015 as DOI: 10.1124/dmd.114.062331
This article has not been copyedited and formatted. The final version may differ from this version.

tissues (heart, lung, stomach, liver, kidney, spleen, small intestine, and large intestine). Protein of DPP-4 was expressed not only in liver but also in other tissues, such as lung, kidney, and small intestine, in mice (Supplemental Fig. 6), which is in agreement with previous reports that human DPP-4 is localized not only in liver but also in other tissues (Mentlein, 1999; Gorrell et al., 2001). It has also been reported that human liver, kidney, and intestinal microsomes are all capable of hydrolyzing vildagliptin to M20.7 in *in vitro* (He et al., 2007). These findings indicate that the hydrolysis of vildagliptin by DPP-4 may occur in whole body in *in vivo* and that the contribution rate of DPP-4 to vildagliptin hydrolysis in humans could be more than 60%.

The DPP-4 activity was determined using the synthetic substrate Gly-Pro-AMC. In our study, the K_m value of the DPP-4 activity in hDPP-4 was approximately 50 μM (Table 2). This K_m value was almost consistent with previous reports (Leiting et al., 2003; Aertgeerts et al., 2005; Lee et al., 2009). Furthermore, the K_m values of the DPP-4 activity in human liver samples were similar to that in hDPP-4 (Table 2). The DPP-4 activity and the protein expression level of DPP-4 in human liver microsomes were higher than those in the human liver cytosol, respectively (Fig. 2A and 2B). DPP-4 has the integral membrane form and soluble form (Durinx et al., 2000). Our findings indicate that liver microsomal fraction abundantly contains a functional DPP-4, which is probably

DMD Fast Forward. Published on January 16, 2015 as DOI: 10.1124/dmd.114.062331
This article has not been copyedited and formatted. The final version may differ from this version.

the membrane form of DPP-4.

The result of inhibition study suggested that the enzyme responsible for the hydrolysis of vildagliptin in human liver was not only DPP-4 (Fig. 4A). Indeed, although the K_m values for high-affinity sites of vildagliptin-hydrolyzing activity in human liver samples were close to that in hDPP-4, the K_m values for low-affinity sites of vildagliptin-hydrolyzing activity in human liver samples were not close to that in hDPP-4 (Table 1). Furthermore, although the protein expression of DPP-4 and the DPP-4 activity in Mock was hardly observed, the vildagliptin-hydrolyzing activity in Mock was observed in a concentration-dependent manner (Supplemental Fig. 7), and the Eadie-Hofstee plots were linear (Supplemental Fig. 2B). The enzyme responsible for the hydrolysis of vildagliptin at the high vildagliptin concentration may be present in human liver samples and the S9 fraction of Mock cells (Table1 and Supplemental Fig. 7). Involvement of multiple enzymes in the cyano group hydrolysis reaction of vildagliptin was first demonstrated in the present study. The C_{max} of vildagliptin after the therapeutic dose of 50 mg twice daily is approximately 1 μM (He, 2012). Human DPP-4 was greatly involved in vildagliptin hydrolysis at 1 μM vildagliptin, whereas the enzymes, which have expressed in Mock cells, were involved in vildagliptin hydrolysis at 50 to 500 μM vildagliptin (Fig. 5D and Supplemental Fig. 7). These

findings also indicate that human DPP-4 could be greatly involved in vildagliptin hydrolysis in *in vivo*.

The result of inhibition study using rat liver S9 fraction (Fig. 4A), which suggested that DPP-4 mainly contributes to the hydrolysis of vildagliptin in rats, was not consistent with the previous report, which suggested that approximately 20% of the formation of M20.7 in rats is likely attributable to DPP-4 (He et al., 2009b). This inconsistency might be due to the fact that the two sets of studies are very different experimental designs. To understand the pharmacokinetics of vildagliptin in humans and other animals, the exploration of multiple enzymes responsible for hydrolysis of vildagliptin needs to be conducted in the future.

We examined the effects of two DPP-4 mutants, R623Q and S630A, on DPP-4 activity and vildagliptin-hydrolyzing activity. It has been reported that vildagliptin forms a reversible covalent bounds with DPP-4 to inhibit DPP-4 enzymatic activity (Ahrén et al., 2011). The covalent binding between vildagliptin and DPP-4 is a consequence of the formation of an unstable complex by reaction of the cyano group of vildagliptin with amino acid residue serine 630 within the catalytic domain of DPP-4 (Potashman et al., 2009; Ahrén et al., 2011). It has been suggested that the amino acid residue serine 630 of DPP-4 is involved in formation of M20.7 (He et al.,

2009a; Ahrén et al., 2011). In the present study, we demonstrated that the catalytic serine 630 residue is directly involved in the vildagliptin hydrolysis in human DPP-4 using S630A-expressing HEK293 cells (Fig. 5D). We also assessed the effects of R623Q, which is the non-synonymous human DPP-4 SNP, on DPP-4 activity and vildagliptin-hydrolyzing activity. Interestingly, although DPP-4 activity in HEK/R623Q was comparable with that in HEK/DPP-4, M20.7 formation rate in HEK/R623Q was statistically lower than that in HEK/DPP-4 ($P < 0.01$) (Fig. 5B and 5D). This reduction of M20.7 formation rate in HEK/R623Q may be due to the influence that the position of its mutation is near to the catalytic serine 630 residue of DPP-4. These results suggest that the DPP-4 genetic polymorphism leads to a decrease of the vildagliptin-hydrolyzing activity.

In conclusion, DPP-4 was greatly involved in vildagliptin hydrolysis in mouse, rat, and human liver. The contribution rate of DPP-4 to vildagliptin hydrolysis in human liver was approximately 60%. Additionally, R623Q mutant, which is the non-synonymous SNP of human DPP-4, led to a decrease of the vildagliptin-hydrolyzing activity. There have been rare cases of hepatic dysfunction in patients treated with vildagliptin (Deacon, 2011; Karagiannis et al., 2014; Kurita et al., 2014). Our findings might be useful for the prediction of liver injury induced by

vildagliptin.

Authorship Contributions:

Participated in research design: Asakura, Fujii, Atsuda, Itoh, and Fujiwara.

Conducted experiments: Asakura and Fujiwara.

Performed data analysis: Asakura and Fujiwara.

Wrote or contributed to the writing of the manuscript: Asakura, Fujii, Atsuda, Itoh, and Fujiwara.

References

Aertgeerts K, Levin I, Shi L, Snell GP, Jennings A, Prasad GS, Zhang Y, Kraus ML, Salakian S, Sridhar V, Wijnands R, and Tennant MG (2005) Structural and kinetic analysis of the substrate specificity of human fibroblast activation protein alpha. *J Biol Chem* **280**: 19441-19444.

Ahrén B, Schweizer A, Dejager S, Villhauer EB, Dunning BE, and Foley JE (2011) Mechanisms of action of the dipeptidyl peptidase□4 inhibitor vildagliptin in humans. *Diabetes Obes Metab* **13**: 775-783.

Akabane T, Gerst N, Naritomi Y, Masters JN, and Tamura K (2012) A practical and direct comparison of intrinsic metabolic clearance of several non-CYP enzyme substrates in freshly isolated and cryopreserved hepatocytes. *Drug Metab Pharmacokinet* **27**: 181-191.

Asakura M, Nakano M, Hayashida K, Fujii H, Nakajima M, Atsuda K, Itoh T, and Fujiwara R (2014) Human nitrilase-like protein does not catalyze the hydrolysis of vildagliptin. *Drug Metab Pharmacokinet* **29**: 463-469.

Boonacker E, and Van Noorden CJ (2003) The multifunctional or moonlighting protein CD26/DPPIV. *Eur J Cell Biol* **82**: 53-73.

Deacon CF (2011) Dipeptidyl peptidase-4 inhibitors in the treatment of type 2 diabetes: a comparative review. *Diabetes Obes Metab* **13**: 7-18.

Durinx C, Lambeir AM, Bosmans E, Falmagne JB, Berghmans R, Haemers A, Scharpé S, and De Meester I (2000) Molecular characterization of dipeptidyl peptidase activity in serum. *Eur J Biochem* **267**: 5608-5613.

Fukami T, and Yokoi T (2012) The emerging role of human esterases. *Drug Metab Pharmacokinet* **27**: 466-477.

Furuta S, Smart C, Hackett A, Benning R, and Warrington S (2013) Pharmacokinetics and metabolism of [14C] anagliptin, a novel dipeptidyl peptidase-4 inhibitor, in humans. *Xenobiotica* **43**: 432-442.

Golightly LK, Drayna CC, and McDermott MT (2012) Comparative clinical pharmacokinetics of dipeptidyl peptidase-4 inhibitors. *Clin Pharmacokinet* **51**: 501-514.

Gorrell MD, Gysbers V, and McCaughan GW (2001) CD26: a multifunctional integral membrane and secreted protein of activated lymphocytes. *Scand J Immunol* **54**: 249-264.

Greene RJ, Tu H, Gibbs JP, and Greg Slatter J (2011) Target-mediated metabolism and target-mediated drug disposition of the DPPIV inhibitor AMG 222. *Xenobiotica* **41**: 945-957.

He YL, Sabo R, Campestrini J, Wang Y, Ligueros-Saylan M, Lasseter KC, Dilzer SC, Howard D, and Dole WP (2007) The influence of hepatic impairment on the pharmacokinetics of the dipeptidyl peptidase IV (DPP-4) inhibitor vildagliptin. *Eur J Clin Pharmacol* **63**: 677-686.

He H, Tran P, Yin H, Smith H, Batard Y, Wang L, Einolf H, Gu H, Mangold JB, Fischer V, and Howard D (2009a) Absorption, metabolism, and excretion of [14C] vildagliptin, a novel dipeptidyl peptidase 4 inhibitor, in humans. *Drug Metab Dispos* **37**: 536-544.

He H, Tran P, Yin H, Smith H, Flood D, Kramp R, Filipeck R, Fischer V, and Howard D (2009b) Disposition of vildagliptin, a novel dipeptidyl peptidase 4 inhibitor, in rats and dogs. *Drug Metab Dispos* **37**: 545-554.

He YL (2012) Clinical pharmacokinetics and pharmacodynamics of vildagliptin. *Clin Pharmacokinet* **51**: 147-162.

Karagiannis T, Boura P, and Tsapas A (2014) Safety of dipeptidyl peptidase 4 inhibitors: a perspective review. *Ther Adv Drug Saf* **5**: 138-146.

Kurita N, Ito T, Shimizu S, Hirata T, and Uchihara H (2014) Idiosyncratic Liver Injury Induced by Vildagliptin With Successful Switch to Linagliptin in a Hemodialyzed Diabetic Patient. *Diabetes Care* **37**: e198-e199.

Lee KN, Jackson KW, Terzyan S, Christiansen VJ, and McKee PA (2009) Using substrate

specificity of antiplasmin-cleaving enzyme for fibroblast activation protein inhibitor design. *Biochemistry* **48**: 5149-5158.

Leiting B, Pryor K, Wu J, Marsilio F, Patel R, Craik CS, Ellman JA, Cummings RT, and Thornberry N (2003) Catalytic properties and inhibition of proline-specific dipeptidyl peptidases II, IV and VII. *Biochem J* **371**: 525-532.

Mentlein R (1999) Dipeptidyl-peptidase IV (CD26)-role in the inactivation of regulatory peptides. *Regul pept* **85**: 9-24.

Metzler WJ, Yanchunas J, Weigelt C, Kish K, Klei HE, Xie D, Zhang Y, Corbett M, Tamura JK, He B, Hamann LG, Kirby MS, and Marcinkeviciene J (2008) Involvement of DPP□IV catalytic residues in enzyme–saxagliptin complex formation. *Protein Sci* **17**: 240-250.

Meunier B, De Visser SP, and Shaik S (2004) Mechanism of oxidation reactions catalyzed by cytochrome P450 enzymes. *Chem Rev* **104**: 3947-3980.

Nagai N (2010) Drug Interaction Studies on New Drug Applications: Current Situations and Regulatory Views in Japan. *Drug Metab Pharmacokinet* **25**: 3-15.

Potashman MH, and Duggan ME (2009) Covalent modifiers: an orthogonal approach to drug design. *J Med Chem* **52**: 1231-1246.

Scheen AJ (2010a) Pharmacokinetics of dipeptidylpeptidase□4 inhibitors. *Diabetes Obes Metab* **12**: 648-658.

Scheen AJ (2010b) Dipeptidylpeptidase-4 inhibitors (gliptins). *Clin Pharmacokinet* **49**: 573-588.

Tanaka T, Kameoka J, Yaron A, Schlossman SF, and Morimoto C (1993) The costimulatory activity of the CD26 antigen requires dipeptidyl peptidase IV enzymatic activity. *Proc Natl Acad Sci USA* **90**: 4586-4590.

Villhauer EB, Brinkman JA, Naderi GB, Burkey BF, Dunning BE, Prasad K, Mangold BL,

Russell ME, and Hughes TE (2003) 1-[[(3-hydroxy-1-adamantyl) amino] acetyl]-2-cyano-(S)-pyrrolidine: a potent, selective, and orally bioavailable dipeptidyl peptidase IV inhibitor with antihyperglycemic properties. *J Med Chem* **46**: 2774-2789.

DMD Fast Forward. Published on January 16, 2015 as DOI: 10.1124/dmd.114.062331
This article has not been copyedited and formatted. The final version may differ from this version.

Legends for Figures

Figure 1. Vildagliptin-hydrolyzing activity of mouse, rat, and human liver samples. (A) The vildagliptin-hydrolyzing activity of mouse, rat, and human liver samples was measured. The substrate concentration was 10 μM. The concentration of M20.7 obtained with the non-reaction control was subtracted from that obtained with each enzyme source. The vildagliptin-hydrolyzing activity was expressed as an M20.7 formation rate (pmol/h/mg protein). Data represent the means ± S.D. of triplicate determinations. **, $P < 0.01$. (B) The substrate concentration-velocity curves of vildagliptin-hydrolyzing activities are shown. Data represent the means ± S.D. of triplicate determinations.

Figure 2. DPP-4 activities and protein expression levels of DPP-4 in mouse, rat, and human liver samples. (A) DPP-4 activity of mouse, rat, and human liver samples was measured using a Gly-Pro-AMC as a substrate. Data represent the means ± S.D. of triplicate determinations. *, $P < 0.05$; **, $P < 0.01$. (B) Mouse, rat, and human liver samples (100 μg of protein) were subjected to NuPAGE 4-12% Bis-Tris Gel and probed with the anti-DPP-4 antibody. GAPDH was used as the protein loading control. (C) The substrate concentration-velocity curves of DPP-4 activities are

shown. Data represent the means ± S.D. of triplicate determinations.

Figure 3. Correlation between M20.7 formation rates and DPP-4 activities in the liver samples. Nine data points for each liver fraction (S9 fraction, cytosol, and microsomes) of three species (mouse, rat, and human) were employed to show the correlation between M20.7 formation rates and the DPP-4 activities. The correlation analysis was preformed using the Spearman rank method. Data represent the means of triplicate determinations.

Figure 4. Inhibition study of vildagliptin-hydrolyzing activity. (A) The inhibitory effect of sitagliptin, a selective DPP-4 inhibitor, on vildagliptin-hydrolyzing activity of mouse, rat, and human liver S9 fractions was assessed. (B) The inhibitory effect of bis(*p*-nitrophenyl) phosphate (BNPP) and ethopropazine, a carboxylesterase and butyrylcholinesterase inhibitor, respectively, on vildagliptin-hydrolyzing activity of human liver S9 fractions was also assessed. The substrate concentration was 10 μM. Data represent the means of triplicate determinations.

Figure 5. Effects of DPP-4 mutants on DPP-4 activity and vildagliptin-hydrolyzing

activity. Stable single expression systems of wild-type human DPP-4, R623Q, and S630A in HEK293 cells (HEK/DPP-4, HEK/R623Q, and HEK/S630A) were constructed. (A) The S9 fraction of Mock, HEK/DPP-4, HEK/R623Q, and HEK/S630A (3 μg of protein) were subjected to NuPAGE 4-12% Bis-Tris Gel and probed with the anti-DPP-4 antibody. Actin was used as the protein loading control. (B) DPP-4 activity of HEK/DPP-4, HEK/R623Q, and HEK/S630A was measured using Gly-Pro-AMC as a substrate. Data represent the means ± S.D. of triplicate determinations. (C) The substrate concentration-velocity curves of DPP-4 activities are shown. The DPP-4 activity in wild-type hDPP-4 and hR623Q was expressed as the DPP-4 activity (nmol/min/mg protein) in which the DPP-4 activity obtained with Mock was subtracted from that obtained with HEK/DPP-4 and HEK/R623Q, respectively. Data represent the means ± S.D. of triplicate determinations. (D) The vildagliptin-hydrolyzing activity of HEK/DPP-4, HEK/R623Q, and HEK/S630A was measured. The substrate concentration was 1 μM. Data represent the means ± S.D. of triplicate determinations. **, $P < 0.01$. (E) The substrate concentration-velocity curves of vildagliptin-hydrolyzing activities are shown. The vildagliptin-hydrolyzing activity in hDPP-4 was expressed as an M20.7 formation rate (pmol/h/mg protein) in which the vildagliptin-hydrolyzing activity obtained with Mock was subtracted from that obtained with

HEK/DPP-4. Data represent the means ± S.D. of triplicate determinations.

Figure 6. Proposed metabolic pathways of vildagliptin in humans. The major metabolic pathway of vildagliptin in humans is hydrolysis at the cyano group to produce a carboxylic acid metabolite M20.7. Vildagliptin is also metabolized to from amide bond hydrolysis (M15.3) and glucuronidation (M20.2). Reported amount of vildagliptin and metabolites in urine and feces is indicated as percentage of dose (He et al., 2009a).

DMD Fast Forward. Published on January 16, 2015 as DOI: 10.1124/dmd.114.062331
This article has not been copyedited and formatted. The final version may differ from this version.

Table 1 Kinetic parameters of vildagliptin-hydrolyzing activity

Enzyme source	Affinity site	K_m	V_{max}
		μM	pmol/h/mg protein
Human liver S9 fraction[a]	High	1.95 ± 0.57	0.25 ± 0.04
	Low	335 ± 9.59	4.97 ± 0.10
Human liver cytosol[a]	High	2.34 ± 0.96	0.18 ± 0.04
	Low	189 ± 5.04	3.18 ± 0.07
Human liver microsomes[a]	High	0.75 ± 0.42	0.69 ± 0.08
	Low	448 ± 104	10.8 ± 2.82
hDPP-4[b]	High	0.62 ± 0.10	11.4 ± 0.79
	Low	151 ± 71.2	11.5 ± 1.55

[a]Calculated from Eadie-Hofstee plots.

[b]Calculated using biphasic equation.

DMD Fast Forward. Published on January 16, 2015 as DOI: 10.1124/dmd.114.062331
This article has not been copyedited and formatted. The final version may differ from this version.

Table 2. Kinetic parameters of DPP-4 activity using Gly-Pro-AMC

Enzyme source	K_m	V_{max}
	μM	nmol/min/mg protein
Human liver S9 fraction	26.2 ± 2.48	2.70 ± 0.16
Human liver cytosol	21.3 ± 1.53	1.71 ± 0.06
Human liver microsomes	24.6 ± 1.11	5.06 ± 0.18
Wild-type hDPP-4	54.0 ± 2.59	281 ± 11.0
hR623Q	45.6 ± 8.03	251 ± 12.6

Figure 1

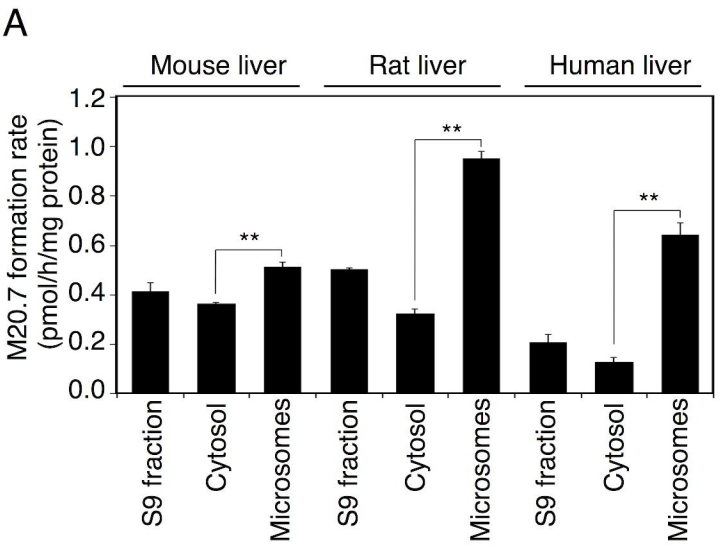
A
Mouse liver
Rat liver
Human liver
M20.7 formation rate (pmol/h/mg protein)
1.2
1.0
0.8
0.6
0.4
0.2
0.0
**
**
**
S9 fraction
Cytosol
Microsomes
S9 fraction
Cytosol
Microsomes
S9 fraction
Cytosol
Microsomes

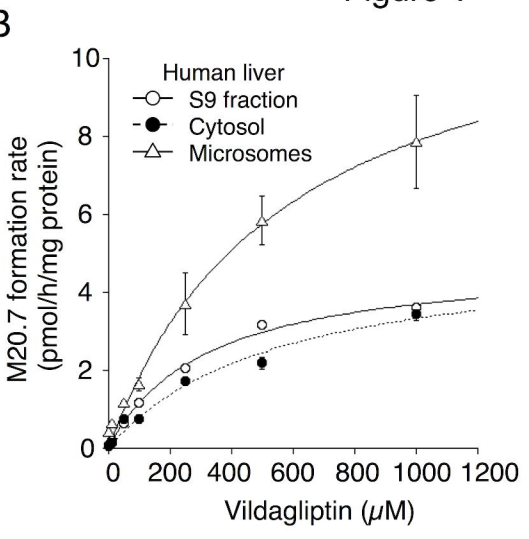
B
Human liver
S9 fraction
Cytosol
Microsomes
M20.7 formation rate (pmol/h/mg protein)
10
8
6
4
2
0
0
200
400
600
800
1000
1200
Vildagliptin (μM)

Figure 2

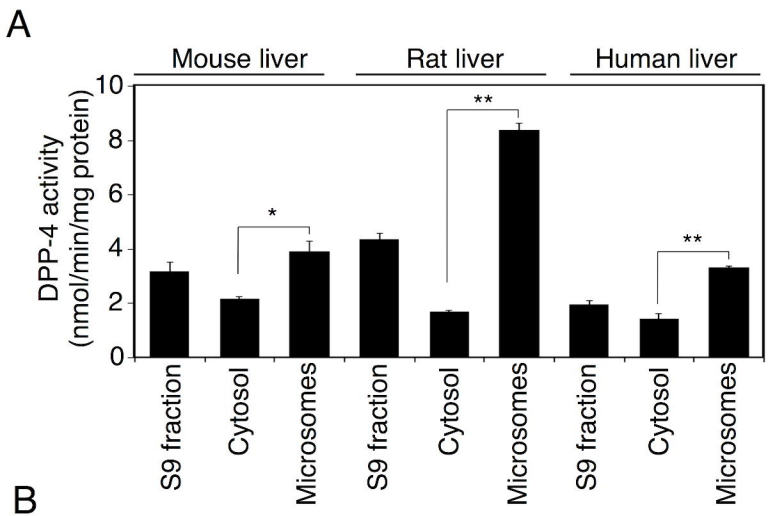
A
Mouse liver
Rat liver
Human liver
DPP-4 activity
(nmol/min/mg protein)
10
8
6
4
2
0
*
**
**
S9 fraction
Cytosol
Microsomes
S9 fraction
Cytosol
Microsomes
S9 fraction
Cytosol
Microsomes

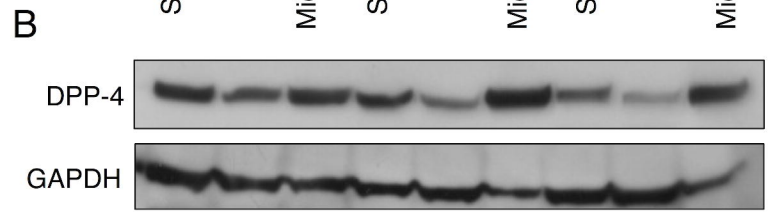
B
DPP-4
GAPDH

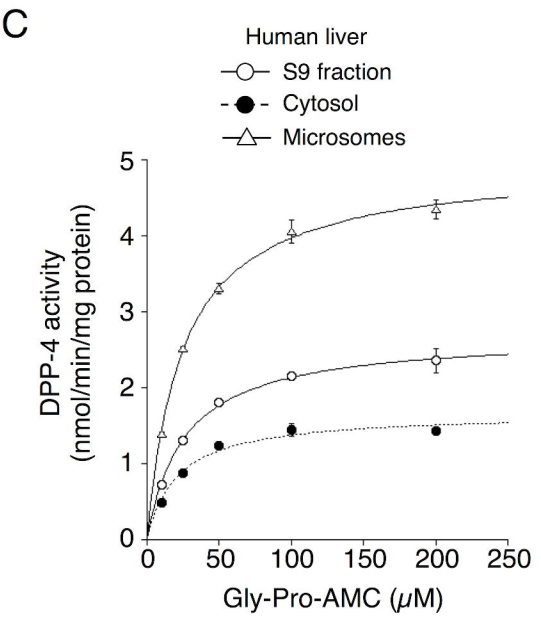
C
Human liver
S9 fraction
Cytosol
Microsomes
DPP-4 activity
(nmol/min/mg protein)
5
4
3
2
1
0
0
50
100
150
200
250
Gly-Pro-AMC (μM)

Figure 3

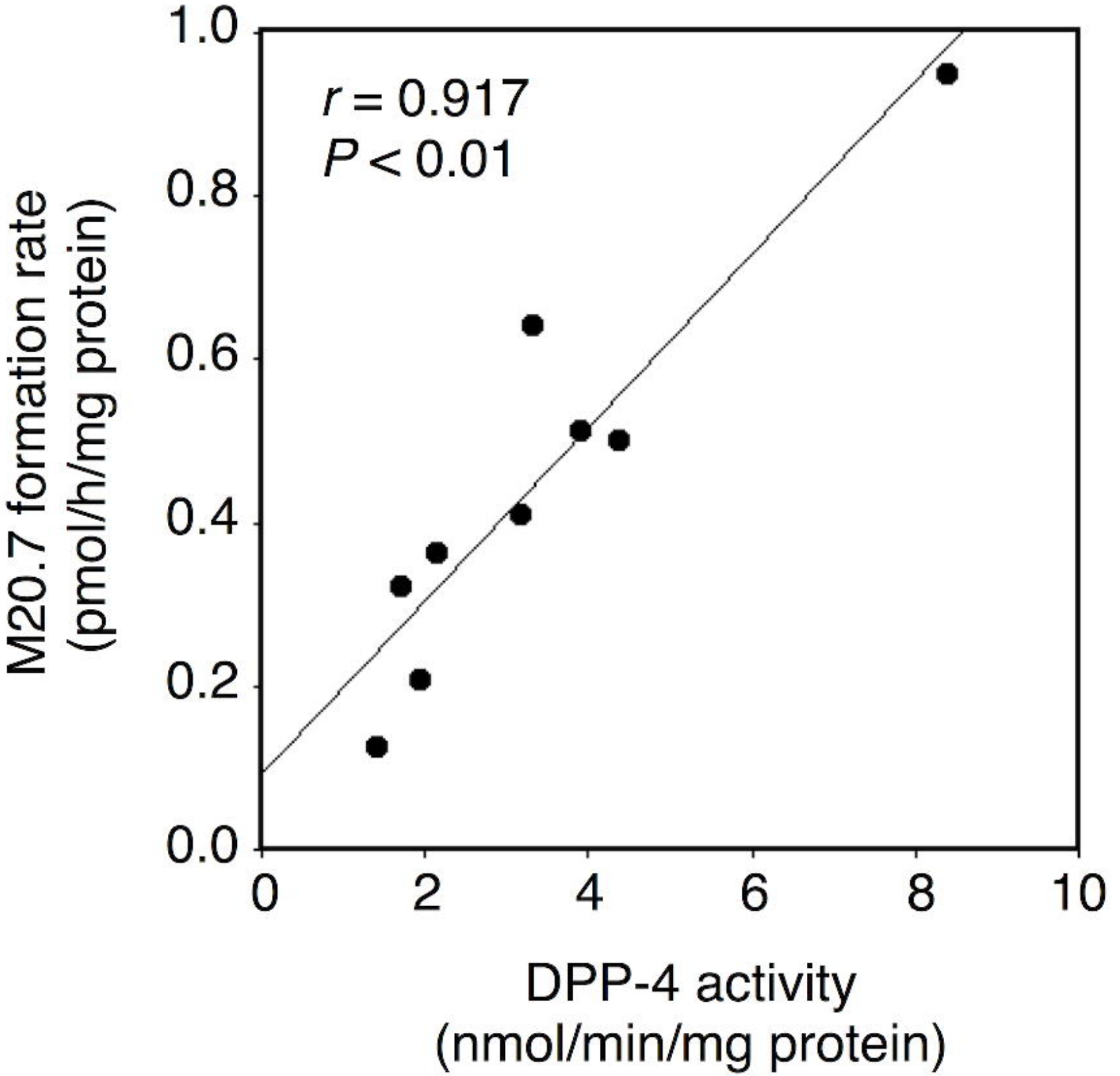
1.0
0.8
0.6
0.4
0.2
0.0
0
2
4
6
8
10
r = 0.917
P < 0.01
M20.7 formation rate
(pmol/h/mg protein)
DPP-4 activity
(nmol/min/mg protein)

Figure 4

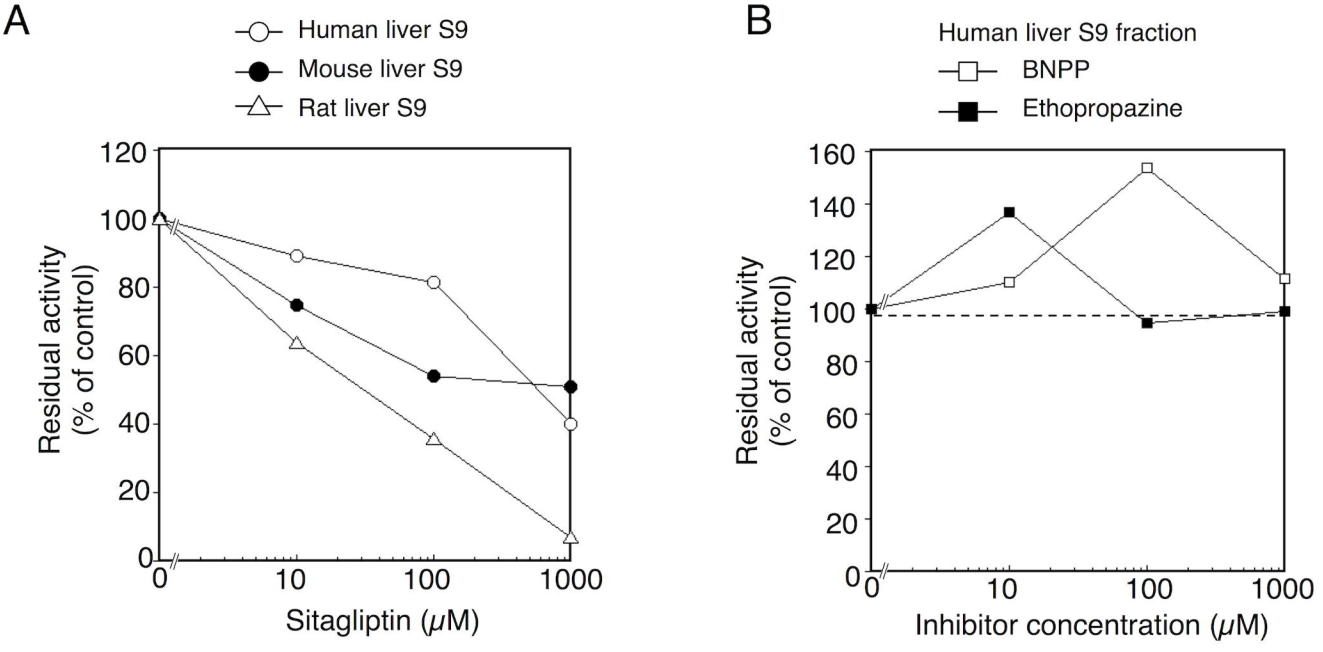
A
Human liver S9
Mouse liver S9
Rat liver S9
Residual activity (% of control)
120
100
80
60
40
20
0
0
10
100
1000
Sitagliptin (μM)
B
Human liver S9 fraction
BNPP
Ethopropazine
Residual activity (% of control)
160
140
120
100
80
60
40
20
0
0
10
100
1000
Inhibitor concentration (μM)

Figure 5

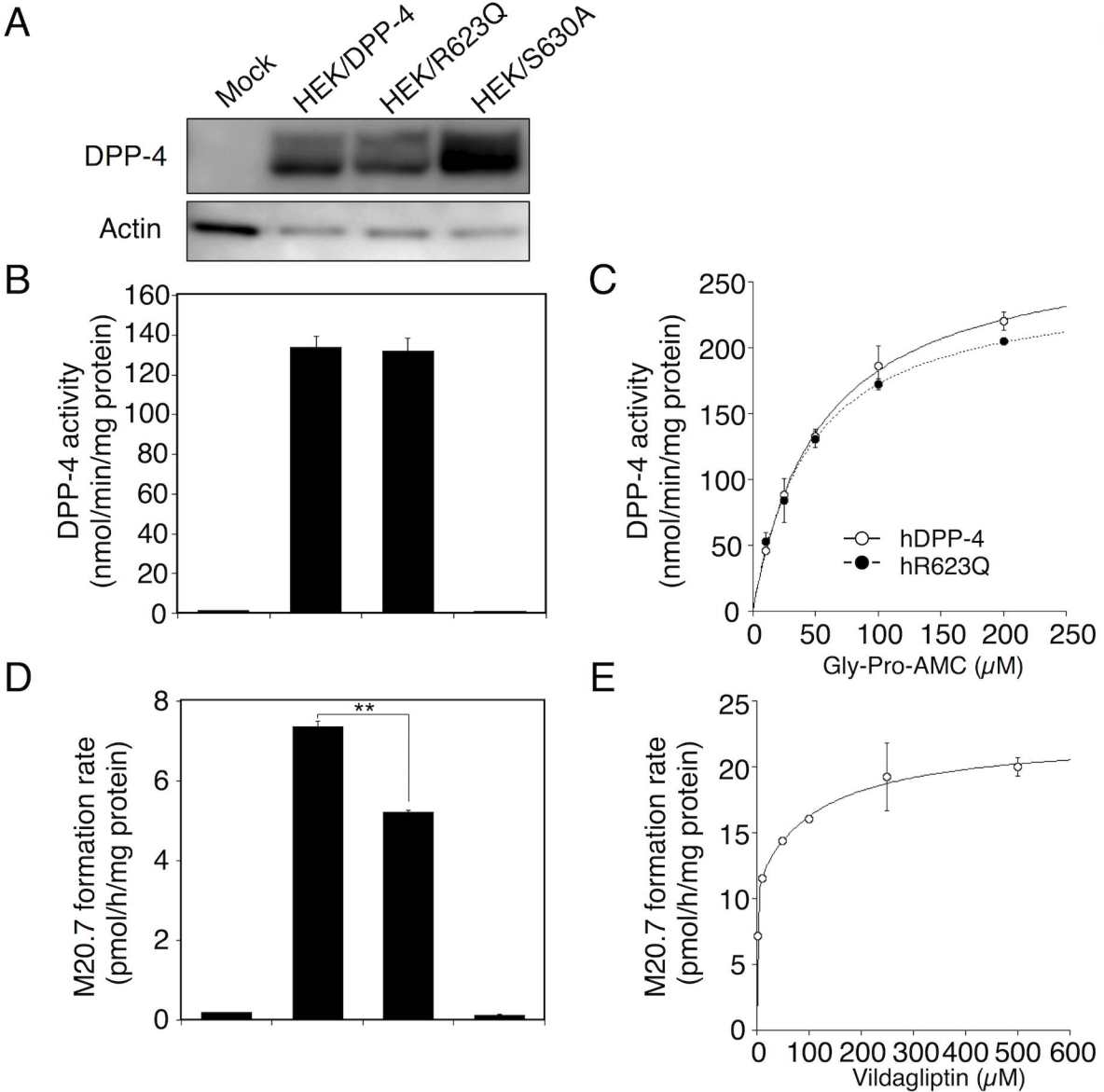
A
Mock
HEK/DPP-4
HEK/R623Q
HEK/S630A
DPP-4
Actin
B
DPP-4 activity
(nmol/min/mg protein)
160
140
120
100
80
60
40
20
0
C
DPP-4 activity
(nmol/min/mg protein)
250
200
150
100
50
0
hDPP-4
hR623Q
0
50
100
150
200
250
Gly-Pro-AMC (μM)
D
M20.7 formation rate
(pmol/h/mg protein)
8
6
4
2
0
**
E
M20.7 formation rate
(pmol/h/mg protein)
25
20
15
10
5
0
0
100
200
300
400
500
600
Vildagliptin (μM)

Figure 6

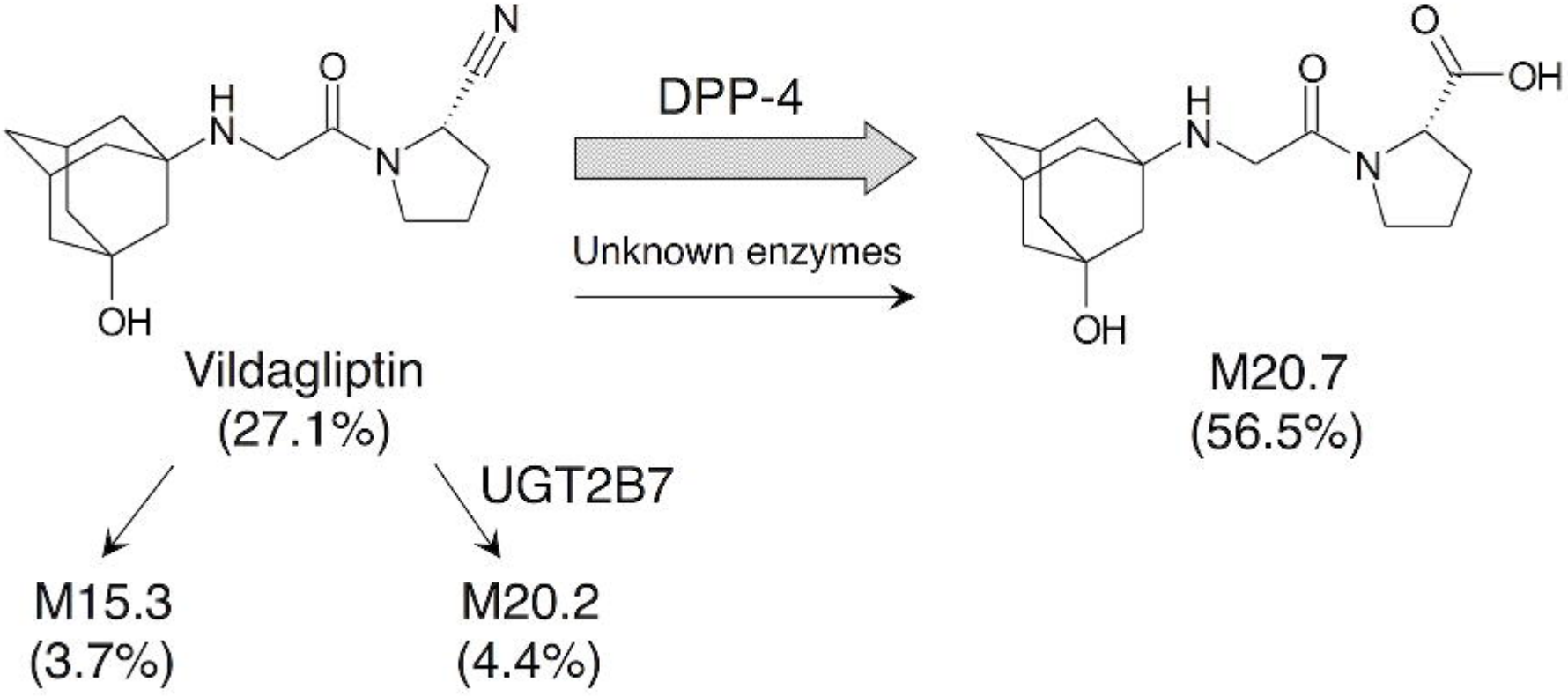
N
O
H
N
N
OH
DPP-4
Unknown enzymes
O
OH
O
H
N
N
OH
Vildagliptin
(27.1%)
M20.7
(56.5%)
UGT2B7
M15.3
(3.7%)
M20.2
(4.4%)